Neurosci Bull June 1, 2015, 31(3): 275–287. http://www.neurosci.cn
DOI: 10.1007/s12264-014-1518-0

·Original Article·

Compromised small-world efficiency of structural brain networks in schizophrenic patients and their unaffected parents

Hao Yan[1,2,3,#], Lin Tian[1,2,3,#], Qifeng Wang[4], Qiang Zhao[5], Weihua Yue[1,2,3], Jun Yan[1,2,3], Bing Liu[4], Dai Zhang[1,2,3,6,7]

[1]*Peking University Six Hospital, Beijing 100191, China*

[2]*Peking University Institute of Mental Health, Beijing 100191, China*

[3]*Key Laboratory of Mental Health, Ministry of Health (Peking University), Beijing 100191, China*

[4]*LIAMA Center for Computational Medicine, National Laboratory of Pattern Recognition, Institute of Automation, Chinese Academy of Sciences, Beijing 100190, China*

[5]*Department of Radiology, The Third Hospital, Peking University, Beijing 100191, China*

[6]*Peking-Tsinghua Center for Life Sciences, Beijing 100871, China*

[7]*PKU-IDG/McGovern Institute for Brain Research, Peking University, Beijing 100871, China*

[#]These authors contributed equally to this work.

Corresponding authors: Hao Yan and Dai Zhang. E-mail: hao_y@bjmu.edu.cn, daizhang@bjmu.edu.cn

ABSTRACT

Several lines of evidence suggest that efficient information integration between brain regions is disrupted in schizophrenia. Abnormalities in white matter tracts that interconnect brain regions may be directly relevant to this pathophysiological process. As a complex mental disorder with high heritability, mapping abnormalities in patients and their first-degree relatives may help to disentangle the risk factors for schizophrenia. We established a weighted network model of white matter connections using diffusion tensor imaging in 25 nuclear families with schizophrenic probands (19 patients and 41 unaffected parents) and two unrelated groups of normal controls (24 controls matched with patients and 26 controls matched with relatives). The patient group showed lower global efficiency and local efficiency. The decreased regional efficiency was localized in hubs such as the bilateral frontal cortices, bilateral anterior cingulate cortices, and left precuneus. The global efficiency was negatively correlated with cognition scores derived from a 5-factor model of schizophrenic psychopathology. We also found that unaffected parents displayed decreased regional efficiency in the right temporal cortices, left supplementary motor area, left superior temporal pole, and left thalamus. The global efficiency tended to be lower in unaffected parents. Our data suggest that (1) the global efficiency loss in neuroanatomical networks may be associated with the cognitive disturbances in schizophrenia; and (2) genetic vulnerability to schizophrenia may influence the anatomical organization of an individual's brain networks.

Keywords: network analysis; diffusion tensor imaging; tractography; white matter; small-world architecture

INTRODUCTION

Over the last decade, graph theoretical analysis of neuroimaging data has provided a useful framework for studies of brain network organization in health and disease[1, 2]. Studies have shown that functional and structural brain networks in humans are highly efficient small-world architectures with high global and local

efficiency of parallel information processing[3-5]. Furthermore, previous studies have demonstrated that the small-world properties of networks derived from neuroimaging data are altered in patients with schizophrenia[6-8]. For example, studies using diffusion tensor imaging (DTI) coupled with whole-brain tractography have revealed disrupted axonal connectivity and reduced network efficiency of the frontal, temporal, and occipital regions in schizophrenia[9, 10]. Impairment of fiber tracts, e.g. reduction in axonal number or density, may diminish the speed at which information is transferred between a pair of cortical regions[11]. In terms of the pathophysiology of schizophrenia, these reported network abnormalities fit the popular dysconnectivity theory of schizophrenia, which proposes that the symptoms of schizophrenia arise from abnormalities in neuronal connectivity[12-14].

In our previous study, we examined anatomical brain networks in schizophrenic patients and normal controls using DTI, demonstrating that the topological properties of the patients' anatomical networks are altered[15]. Since schizophrenia is believed to be a complex mental disorder, mapping abnormalities in patients may not fully disentangle the risk factors involved in its development[16]. One of the main strategies devised to address this issue is to focus investigations of network abnormalities on individuals with high genetic risk factors for schizophrenia, such as the unaffected first-degree relatives of patients, mostly siblings[17]. Studying these individuals allows evaluation of the underpinnings of schizophrenia that are independent of the disease state. Many studies have investigated schizophrenic patients and first-degree relatives with DTI, and suggested that patterns of abnormal structural connectivity may be an important endophenotype of schizophrenia[18-22]. Recently, using diffusion-weighted imaging, Collin *et al.* found that the network organization is abnormal in schizophrenia and their unaffected siblings, and suggested that structural connectivity is an indicator of genetic predisposition for schizophrenia[23]. However, to our knowledge, no studies have used graph theoretical analysis to investigate anatomical networks in patients with schizophrenia and their unaffected parents.

Another problem with previous studies of the relationship between altered network measures and clinical variables in schizophrenia is that their findings are equivocal. That is, while some studies reported no correlation between network measures and clinical variables[9], others suggested a negative correlation between the course of illness and loss of network efficiency[6]. Therefore, it is our belief that the correlations between clinical symptoms and structural networks require further consideration.

By establishing a weighted network model of white matter connections using DTI followed by whole-brain tractography as described in our previous study[15], we set out to explore the structural brain networks of both schizophrenic patients and their unaffected biological parents. We focused on network efficiency because it is a suitable scale for characterizing the small-world properties of weighted networks[5, 24]. Previous studies of healthy twins have shown that the characteristic features of small-world networks are genetically mediated[25] and highly heritable[26]. Therefore, we expected that (1) schizophrenic patients would show a significant loss of structural brain network efficiency; and (2) assuming that network efficiency is a heritable trait, it would be found at least in a mild manner in the unaffected parents, who have a genetically enhanced risk for schizophrenia.

MATERIALS AND METHODS

Subjects

Twenty-five nuclear families with schizophrenic probands and 50 normal controls who reported no first- or second-degree relatives with schizophrenia and well-matched with patients or their parents for age, sex, and educational level were recruited through the Institute of Mental Health, Peking University. To improve the homogeneity of our analysis, only schizophrenic patients with the most common paranoid subtype were recruited. Fifteen individuals from 9 families (in the 9 families, at least one family member was included in the subsequent analysis) were excluded from the study because of (1) non-cooperation with the scan (n = 2, all patients); (2) left-handedness (n = 7, 3 patients and 4 parents) evaluated using the Edinburgh Handedness Inventory[27]; and (3) contraindications for magnetic resonance imaging (MRI) (n = 6, 1 patient and 5 parents). Other exclusion criteria were electroconvulsive therapy within 6 months and a history of serious medical illness.

MRI scans were successfully acquired from 110 individuals: 19 schizophrenic patients (SZ), 41 unaffected first-degree relatives (PA), all of whom were biological parents, and 50 normal controls [24 young individuals matched to the probands (NC1) and 26 elderly individuals matching the first-degree relatives of patients (NC2)]. Two trained and experienced psychiatrists ensured that the patients satisfied the ICD-10 diagnostic criteria for research on schizophrenia of the paranoid subtype[28]. At the time of their MRI scans, all patients were receiving antipsychotic medications, the doses of which were converted into chlorpromazine equivalents[29-31]. The disease severity and psychopathology were assessed by an experienced psychiatrist using the Positive and Negative Symptoms Scale (PANSS)[32]. Rather than using the total or subscale scores, we used a 5-factor model of schizophrenic psychopathology (positive: delusion and grandiosity; negative: emotional withdrawal, poor rapport, and social withdrawal; excitement: excitement and hostility; cognition: conceptual disorganization and abstract thinking; depression and anxiety: anxiety, guilt feelings, and depression) to more accurately assess and measure the discrete dimensions of their psychopathology[33]. All participants were assessed to be right-handed using the Edinburgh Handedness Inventory[27] and had no intracranial pathology, history of head injury, neurological disorder, or alcohol/substance abuse. Table 1 lists the demographic and clinical characteristics of the patients, the first-degree relatives, and all normal controls. This study was approved by the Medical Ethics Committee of the Institute of Mental Health, Peking University. All participants were given detailed information regarding the purposes and procedures of the study. Written consent was given by the patients and/or their parents (among whom 2 out-patients with milder symptoms signed the written consent themselves), and all healthy participants enrolled in this study.

MRI Data Acquisition

MRI scans were obtained at the Department of Radiology of the Third Hospital, Peking University, with a 3.0-Tesla Magnetom Trio (Siemens Medical System, Erlangen, Germany). Foam pads were used to reduce head motion and scanner noise. Three-dimensional T1-weighted images were acquired in a sagittal orientation using a 3D-MPRAGE sequence with the following parameters: time repetition (TR) = 2350 ms, time echo (TE) = 3.44 ms, flip angle = 7°, matrix size = 256 × 256, field of view (FOV) = 256 × 256 mm^2, 192 sagittal slices, slice thickness = 1mm, acquisition voxel size = 1.0 × 1.0 × 1.5 mm^3. Diffusion tensor images were acquired using a single-shot echo-planar imaging-based sequence with the following parameters: TR = 5300

Table 1. Demographic and clinical characteristics of the patients, their unaffected parents, and normal controls

Variable	SZ (*n* = 19)	NC1 (*n* = 24)	*P*	PA (*n* = 41)	NC2 (*n* = 26)	*P*
Gender (male/female)	8/11	14/10	0.29[a]	20/21	14/12	0.69[a]
Age (years)	23.4 (4.4)[b]	22.6 (3.4)	0.48[c]	52.2 (7.1)	52.0 (5.9)	0.93[c]
Education (years)	13.6 (1.9)	14.0 (1.9)	0.49[c]	13.3 (3.0)	13.1 (2.7)	0.77[c]
Brain size (voxels)	154,980 (17,825)	155,573 (10,453)	0.90[c]	150,740 (11,459)	147,733 (13,267)	0.33[c]
Course of illness (months)	43.8 (32.9)					
Medication dose (mg/day) [d]	442.5 (293.3)					
Positive[e]	16.8 (3.9)					
Negative[e]	14.8 (4.9)					
Excitement[e]	9.5 (2.8)					
Cognition[e]	8.5 (2.8)					
Depression and anxiety[e]	6.3 (1.8)					

SZ, schizophrenic patients; NC1, normal controls for schizophrenic patients; PA, unaffected parents of schizophrenic patients; NC2, normal controls for parents. [a]Pearson's χ^2 test; [b]mean (standard deviation); [c]two-sample *t*-test; [d]chlorpromazine-equivalent dose; [e]5-factor model of schizophrenic psychopathology as measured by the Positive and Negative Syndrome Scale.

ms, TE = 92 ms, thickness/gap = 3/0.3 mm, matrix = 128 × 128, FOV = 230 × 230 mm^2, acquisition voxel size = 1.8 × 1.8 × 3.0 mm^3, number of excitation = 2, slices = 40, 64 diffusion directions with b = 1000 s/mm^2, and an additional image without diffusion weighting (i.e., b = 0 s/mm^2).

MRI Data Preprocessing

The current study followed the same MRI data preprocessing methods as those described in our previous paper[15]. In brief, the T1-weighted image of each participant was co-registered to his/her non-diffusion-weighted image (b = 0 s/mm^2) using the SPM2 package (http://www.fil.ion.ucl.ac.uk/spm), resulting in a co-registered T1 image in native DTI space. For the diffusion-weighted images, we used the Diffusion Toolbox of FMRIB to correct simple head motion and eddy current distortion (FSL 4.1; http://www.fmrib.ox.ac.uk/fsl). The six independent components of the diffusion tensor and the corresponding FA and eigenvectors were calculated using in-house software named DTI Tracking (http://www.brainnetome.org).

Construction of Weighted Brain Anatomical Connectivity Networks

Definition of Network Node

In order to construct a weighted network for each participant, we followed the method used in a previous study of anatomical brain networks[34]. Specifically, the automated anatomical labeling (AAL) template[35] was used to segment the entire cerebral cortex of each participant into 90 regions (45 for each hemisphere) with the cerebellum excluded. Each region represented a node of the final anatomical network. Each individual co-registered T1 image was normalized to the SPM2 T1 template of Montreal Neurological Institute (MNI) space by applying an affine transformation with 12 degrees of freedom, along with a series of non-linear warps. We then inverted the resulting transformation matrix and used it to warp the AAL template from MNI space to the diffusion MRI native space, in which the discrete labeling values were preserved by a nearest-neighbor interpolation method[34, 36]. With this procedure, 90 cortical and subcortical regions (45 for each hemisphere) were obtained in the DTI native space.

Definition of Network Edge

A deterministic streamline tracking algorithm, the fiber assignment continuous tracking (FACT) algorithm, was used for fiber tracking[37]. The tracking procedure was terminated at voxels with an FA value <0.15 or when the angle between adjacent steps was >45°[34, 38]. If the two end-points of the reconstructed fiber bundles were located within two AAL regions, the two regions were considered to be connected[34, 36].

The number (N_{ij}) of connections between two regions was used to define the weight of the edge:

$$W_{ij} = \begin{cases} \frac{1}{N_{ij}}, & \text{if } N_{ij} \geq T \\ 0, & otherwise \end{cases} \quad (1)$$

Under this definition, W_{ij} is proportional to the distance between two brain regions, which means the larger the connections the shorter the distance. Afterwards, these distance values were used to calculate the shortest path length (L_{ij}) between each pair of nodes using the Dijkstra algorithm, which is similar to the definition used in previous reports[5, 39]. Because false-positive connections could result from using the deterministic streamline tracking algorithm, we used a series of threshold values (T, from 1 to 21) for the number of existing fibers in order to examine the robustness of our construction method. That is, two regions linked with fewer than T fibers were considered disconnected. The threshold values were selected to keep the average size of the largest connected component at 90 across all participants, so that the networks of the majority of participants were fully connected at each threshold value.

Graph Theoretical Analyses of the Weighted Network Properties

Definition of Network Properties

A number of graph metrics were defined to examine the global and local properties of structural brain networks. The global metrics were (1) global efficiency of the network E_{global}; (2) local efficiency of the network E_{local}; and (3) overall connectivity strength S, computed for each participant as the sum of all connections in the network. The node-specific metrics were (1) local efficiency of node i E_{i_local}; and (2) regional efficiency of node i $E_{i\_regional}$.

In the present study, the topological properties used

were as follows: *G* denotes the whole weighted network. G_i is used for the subgraph of node *i*, which is constructed by its direct neighbor nodes and the edges linking these neighbor nodes. *N* represents the total number of nodes in the network. Global efficiency is a measure of the transfer speed of parallel information in a graph and local efficiency is a measure of the information exchange of each subgraph[5].

Global network metrics The global efficiency of the network (E_{global}) measures the global efficiency of parallel information transfer in the network[24], which is defined as the inverse of the harmonic mean of the shortest path length (L_{ij}) between each pair of nodes:

$$E_{global} = \frac{1}{N(N-1)} \sum_{i,j \in G, i \neq j} \frac{1}{L_{ij}} \quad (2)$$

The local efficiency of the whole network (E_{local}) measures the fault tolerance of the network, indicating how well the information is communicated between the neighbors of a given node when that node is removed[5], which is defined as the average of the local efficiency of node *i* (E_{i_local}) across all nodes in the network:

$$E_{local} = \frac{1}{N} \sum_{i \in G} E_{i\_local} \quad (3)$$

Local network metrics The local efficiency of node *i* (E_{i_local},), where *i* = 1, 2,…, 90, is calculated as the global efficiency of G_i:

$$E_{i\_local} = E_{global}(G_i) \quad (4)$$

The regional efficiency of a node quantifies the importance of each node for communication within the network[39]. $E_{i\_regional}$, where *i* = 1, 2,…, 90, is defined as the inverse of the harmonic mean of L_{ij} between node *i* and all other nodes in the network[5]:

$$E_{i\_regional} = \frac{1}{N-1} \sum_{i,j \in G, i \neq j} \frac{1}{L_{ij}} \quad (5)$$

Evaluation of the Small-World Properties

The small-world concept, characterized by path length *L* less than a regular lattice and clustering coefficient *C* greater than a random graph, was originally proposed in a study of binary networks[3]. However, as several previous studies have demonstrated, weighted networks are more suitable for characterizing real world network topology, where E_{global} and E_{local} have been found to be suitable scales for characterizing the small-world properties of weighted networks[5, 24]. Practically speaking, a weighted network can be categorized as small-world if E_{global} is slightly less than and E_{local} is much greater than a matched random network[5, 39]. In the current study, we followed the procedure used by Gong *et al.* to evaluate the small-world properties[39]. In order to preserve the weight distribution of the entire network, we used a Markov-chain algorithm to generate 100 random networks for each individual's network while retaining the weight of each edge. Then we calculated E_{global} and E_{local} across these random networks and compared them with the properties of real networks.

Statistical Analysis

To determine the significant changes of network properties in patients and their first relatives, we compared the global (E_{global}, E_{local}, and S) and node-specific ($E_{regional}$) network metrics between the probands, unaffected parents, and their respective control counterparts; an analysis of covariance (ANCOVA) model with diagnostic group as the fixed variable was conducted separately. Gender, age, and brain size of participants were included as covariates in order to exclude their potential effects[39]. Considering that the global network measures could be influenced by the total level of connectivity S, we did another ANCOVA analysis of E_{global} and E_{local} by adding the S as a potentially confounding variable together with age, gender, and brain size. The threshold value for establishing significance was set at P <0.05 for global network measures (E_{global}, E_{local} and S). To correct for multiple comparisons in the node-specific analysis ($E_{regional}$), *P*-values were subjected to a false-discovery rate (FDR) threshold of q = 0.05. Because the analysis of the regional localization of effects of schizophrenia on network efficiency was exploratory in nature, we also reported the results that survived an uncorrected threshold of P <0.05[9].

A partial correlation analysis that controlled for three potentially confounding variables (age, gender, and brain size) was used to estimate the correlation between the network properties (E_{global} and E_{local}) and clinical variables

(course of illness, medication dose, and total PANSS score along with the 5-factor model of schizophrenic psychopathology). In this exploratory analysis, we used a statistical significance threshold of P <0.05 (uncorrected).

RESULTS

Efficient Small-World Properties of the Four Groups

After comparing the same parameters estimated in a random graph over a range of network connection thresholds, we found that all the participants had a small-world organization of structural brain networks, i.e. they had less global efficiency and greater local efficiency than those of the random graph (Figs. 1 and 2).

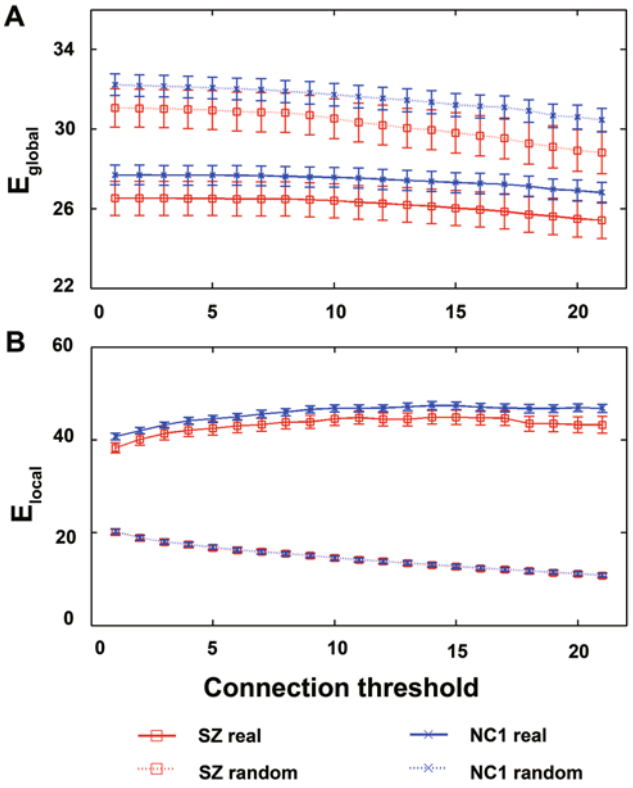

Fig. 1. Efficiency properties of the weighted anatomical network of the normal control group and the schizophrenic patient group. (A) Global and (B) local efficiency are shown as a function of connection threshold for a random graph and real brain networks [(normal controls NC1, blue crosses) and schizophrenic patients (SZ, red squares)]. The global efficiency profiles of the real networks are less than those of random networks, but the local efficiency profiles of the real networks are greater than those of random networks over the connection threshold, known as small-worldness. Error bars correspond to the standard error of the mean.

Between-Group Differences in Network Metrics

Global Network Metrics

The ANCOVA comparing SZ to NC1 revealed that global efficiency E_{global} was significantly lower in SZ over the whole range of connection thresholds (Fig. 3A, Table S1), whereas local efficiency E_{local} was significantly lower in SZ only at nearly half the range of thresholds (Fig. 3B, Table S2). The ANCOVA comparing PA to NC2 revealed that the E_{global} was not significantly different but tended to be lower in PA over the whole range of connection thresholds (Fig. 4A, Table S3), whereas the E_{local} was not significantly altered in PA (Fig. 4B, Table S4). In addition, we found no

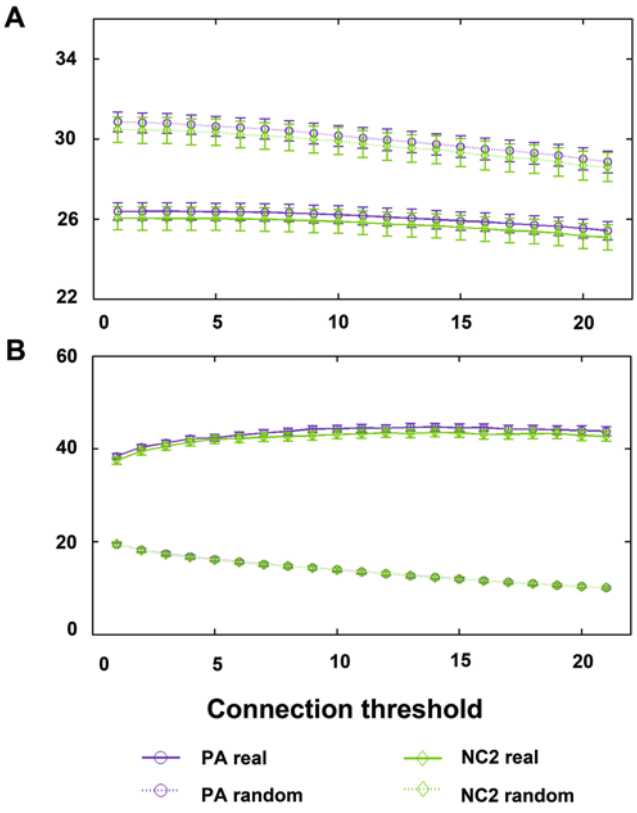

Fig. 2. Efficiency properties of the weighted anatomical network of the normal control group and the first-degree relatives group. (A) Global and (B) local efficiency are shown as a function of connection threshold for a random graph and real brain networks [normal controls (NC2, green rhombuses), the unaffected first-degree relatives (PA, purple circles)]. Error bars correspond to the standard error of the mean.

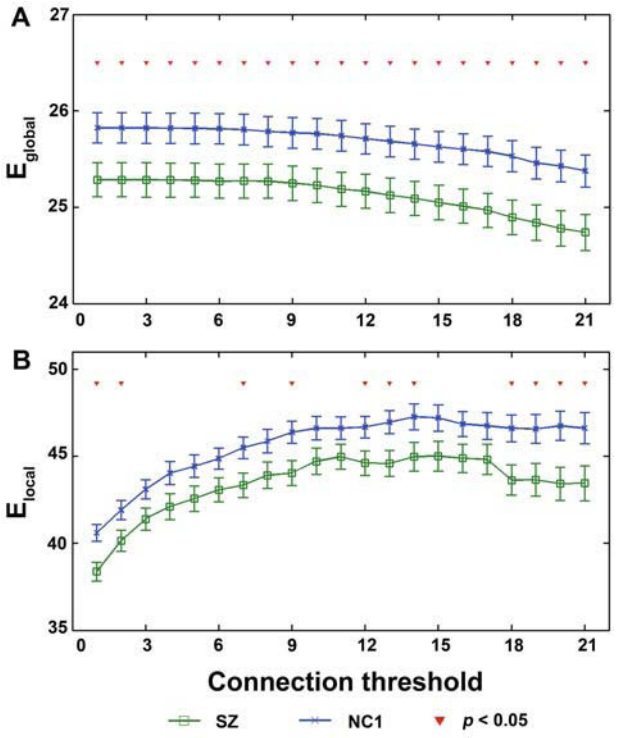

Fig. 3. Mean global efficiency, E_{global} (A), and local efficiency, E_{local} (B), for schizophrenic patients (SZ) and young normal controls (NC1) as a function of connection threshold. Error bars correspond to the standard error of the mean. An analysis of covariance using diagnostic group as the fixed variable with gender, age, and brain size as covariates was performed to test the difference of network measures between groups.

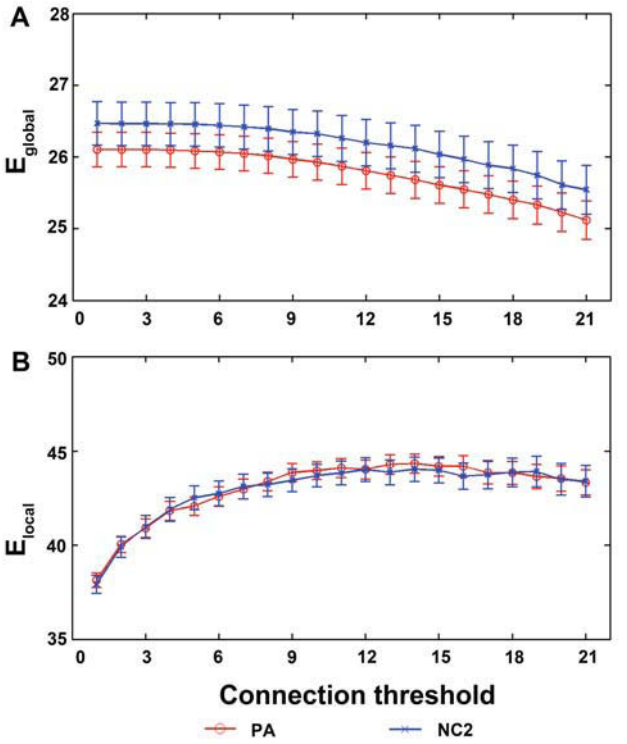

Fig. 4. Mean global efficiency, E_{global} (A), and local efficiency, E_{local} (B), for unaffected first-degree relatives of schizophrenic patients (PA) and elderly normal controls (NC2) as a function of connection threshold. Error bars correspond to the standard error of the mean.

significant changes in the overall connectivity strength S in SZ and PA, compared with their healthy controls (Tables S5 and S6).

When S was added as another potentially confounding variable in ANCOVA analysis of E_{global} and E_{local}, together with age, gender, and brain size, the results were almost the same, but the *P*-value of group comparison of E_{global} between SZ and NC1 became smaller at almost all thresholds (Table S7).

Local Network Metrics

None of the results for the ANCOVA analysis of $E_{regional}$ survived the FDR correction. However, if we set the significance threshold as $P < 0.05$, uncorrected, we found some regions with a trend for decreased regional efficiency in both the SZ and PA groups. The ANCOVA comparing SZ

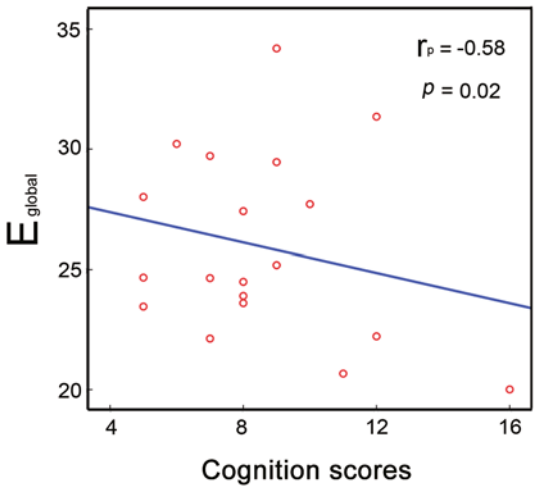

Fig. 5. Mean global efficiency (E_{global}) of structural brain networks against the cognition scores with trend lines in schizophrenic patients. The partial correlation coefficient (r_p) was used to assess the significance of a partial correlation controlled for three potentially confounding variables (age, gender, and brain size).

Table 2. Brain regions with significant differences in adjusted regional efficiency between the schizophrenic group and their controls

Class	Brain region	Mean value (SD)		*P*-value*
		NC1 (*n* = 24)	SCZ (*n* = 19)	
Association	Frontal_Sup_L	43.06 (0.97)	39.61 (1.10)	0.025
	Frontal_Sup_R	42.04 (0.86)	36.70 (0.97)	<0.001
	Frontal_Mid_R	40.67 (0.73)	36.42 (0.82)	<0.001
	Frontal_Inf_Oper_R	29.36 (0.51)	27.41 (0.58)	0.017
	Frontal_Inf_Tri_R	36.72 (0.62)	34.47 (0.69)	0.022
	Frontal_Sup_Medial_L	35.01 (0.73)	31.69 (0.82)	0.005
	Frontal_Sup_Medial_R	36.46 (0.88)	32.24 (0.99)	0.003
	Cingulum_Ant_L	28.36 (0.59)	25.70 (0.67)	0.006
	Cingulum_Ant_R	30.85 (0.66)	28.78 (0.75)	0.047
	Parietal_Inf_R	11.22 (0.78)	8.64 (0.88)	0.036
	SupraMarginal_R	21.54 (0.58)	18.04 (0.65)	<0.001
	Precuneus_L	23.52 (0.55)	21.07 (0.62)	0.006
Paralimbic/Limbic	Cingulum_Post_R	18.41 (0.56)	16.46 (0.63)	0.026

*Uncorrected *P*-values (calculated using a general linear model after adjusting for the effects of gender, age, and brain size). L, left; R, right; Inf, inferior; Ant, anterior; Post, posterior; Mid, middle; Sup, superior; Tri, triangle; Oper, opercular; SD, standard deviation.

Table 3. Brain regions with significant differences in adjusted regional efficiency between the unaffected parents of schizophrenic patients and their controls

Class	Brain Region	Mean Value (SD)		*P*-value*
		NC2 (*n* = 26)	Relatives (*n* = 41)	
Association	Supp_Motor_Area_L	32.13 (0.89)	29.57 (0.70)	0.029
	Temporal_Sup_R	29.43 (0.75)	27.25 (0.60)	0.028
	Temporal_Mid_R	28.57 (0.71)	26.68 (0.56)	0.042
Subcortical	Thalamus_L	29.37 (0.63)	31.23 (0.50)	0.025
Paralimbic/Limbic	Temporal_Pole_Sup_L	32.61 (0.80)	30.42 (0.64)	0.038

*Uncorrected *P*-values (calculated using a general linear model after adjusting for the effects of gender, age, and brain size). L, left; R, right; Mid, middle; Sup, superior; SD, standard deviation.

to NC1 revealed decreased regional efficiency $E_{regional}$ in a number of SZ brain regions, including the superior frontal cortices, anterior cingulate cortices, and right posterior cingulate cortex (Table 2). The ANCOVA comparing PA to NC2 revealed decreased regional efficiency in several PA brain regions, including the right superior and middle temporal cortex, left supplementary motor area, left superior temporal pole, and left thalamus (Table 3).

Relationship between Network Measures and Clinical Variables

Linear correlations were found between clinical variables

and attributes of network organization (Fig. S1) in the SZ group. In particular, we found that the global efficiency was negatively correlated with cognition scores derived from schizophrenic psychopathology over the whole range of connection threshold values (Table S8). We showed the patterns at a moderate connection threshold of 16 (Fig. 5).

DISCUSSION

In this study, we characterized the anatomical disorganization of brain networks in both schizophrenic patients and their unaffected parents using graph theoretical analysis. We found that the structural networks in the members of proband families and normal controls had salient small-world properties (Figs. 1 and 2). This finding is consistent with previous studies, which suggested that key aspects of cortical structural organization are highly conserved in members of families affected by schizophrenia[8, 9, 15].

Although the structural networks retained their small-world properties regardless of schizophrenia, their underlying global organization was altered in patients, who displayed lower global and local efficiency. These findings are consistent with studies that have modeled structural connectivity disturbances across the entire brain of patients with schizophrenia[9, 10], and suggested that schizophrenia-related connectivity impairments are not exclusive to synaptic abnormalities, but are also implicated in alterations of white matter tracts on a macro-scale. When considered in the context of previous findings from functional MRI data[6, 40, 41], in which network efficiency loss has also been found in schizophrenic patients, the current results suggested that both the functional and anatomical organization of brain networks are disrupted in schizophrenia. The results are further evidence that there is insufficient and/or ineffective communication between brain regions in schizophrenia. In the current study, patients also showed lower regional efficiency in selective cortical regions, including the frontal and parietal gyri and cingulate cortex. Given that these findings did not survive multiple-comparison correction, the alteration of node-specific network metrics in patients should be interpreted as preliminary. However, what we found was highly consistent with the findings of previous studies[9, 10]. For example, Van den Heuvel *et al.* reported longer structural path lengths in the right inferior frontal cortex, right anterior cingulate cortex, and left middle frontal cortex in schizophrenia, suggesting reduced regional efficiency in these regions[9]. The regional efficiency of each node is a measure of its connectivity to all other nodes of the network; highly-connected nodes have high regional efficiency. The reduced regional efficiency suggests that schizophrenia impacts the capacity of the frontal and cingulate regions to efficiently integrate information across the brain network, an impairment that is especially important considering that the frontal and cingulate regions have been identified as the most highly-connected brain regions ('hubs')[8, 41, 42]. Here, a hub refers to a node occupying a central position in the overall organization of a network[43]. Functional and anatomical connectivity studies have confirmed that the frontal and parietal hubs play a less central role in patients with schizophrenia[23, 44]. And the altered organization of hub nodes in schizophrenia has been suggested to be a critical factor in determining the topological alterations of the overall network[9, 23].

The specific properties of brain network organization have functional importance[10], and their alterations might provide clinically useful diagnostic markers for neuropsychiatric disease[45]. In the present study, a negative correlation between global network efficiency and cognition scores derived from schizophrenic psychopathology was found. There is evidence of slowed cognitive processing in schizophrenic patients, likely contributing to deficits in domains that rely on the rapid and efficient assimilation of information[46]. In addition, in healthy adults, better cognitive function has been associated with the increased global efficiency of their brain network organization in data from functional MRI[47] and magnetoencephalography[48]. Although no neuropsychological testing was used to assess cognitive function in the current study, previous studies have shown that cognitive function assessed with cognition subscales derived from symptom assessment has approximately the same predictive ability for activities of daily living in patients as cognitive function that is measured with comprehensive batteries of neuropsychological testing[49]. Thus, the negative correlation between cognition scores and network global efficiency in our study indicates that a loss of global efficiency in neuroanatomical networks appears to be one of the underlying mechanisms responsible for the cognitive

disturbances in schizophrenia. Undoubtedly, more studies with increased numbers of participants using specific neuropsychological tests or cognitive tasks are needed to confirm this finding.

Another important goal of the study was to explore the small-world structural brain networks in first-degree relatives of schizophrenic patients. We found that unaffected parents showed decreased regional efficiency in the right temporal cortex, left supplementary motor area, left superior temporal pole, and left thalamus. The explanation for this phenomenon is unclear because previous DTI studies that included high-risk individuals are relatively rare and inconsistent. This lack of consistent findings is likely due to methodological factors. For example, two voxel-based analysis studies reported FA changes in temporo-frontal white matter regions in high-risk individuals[18, 50], whereas a tractography study reported no such changes[51]. However, the current results permit speculation about the role of genetic factors in schizophrenia. Previous studies have demonstrated that individuals at high risk for schizophrenia may have genetically-associated gray-matter alterations in the temporal lobe[52] and thalamus[53], regions where we also found impaired network efficiency. While no abnormalities in frontal regions were found in parents, the temporal lobe is another hub with high lesion probability in schizophrenia[43]. Twin and family studies have shown that the organization of structural and functional brain networks is under genetic control[54, 55]. Therefore, these findings provide evidence for the perspective that core components of the vulnerability to schizophrenia target specific brain regions[56]. Our study also found that global efficiency tended to be lower in the parents of patients. This finding is in keeping with previous structural and functional MRI studies, in which unaffected first-degree relatives show a pattern of brain abnormalities similar to but milder than those in schizophrenic patients[17]. This could indicate that genetic influences on the anatomical disorganization of brain networks increase an individual's vulnerability to schizophrenia.

Some issues should be considered when interpreting the findings of the current study. We found no significant between-group differences of S in all 21 thresholds (Tables S5 and S6), which was not completely inconsistent with a previous study[23]. In that study, they found differences of S between patients and controls, but no differences between siblings and controls. We thought the thresholds we selected might be one of the reasons that no differences of S were found in the four groups. Because the majority of participants were fully connected in the selected thresholds, the effect size of S may not have been large enough to reflect the connectivity issue of patients. Considering that the overall connectivity strength S might have a pronounced effect on other network metrics, we did another ANCOVA analysis of E_{global} and E_{local} by adding the S as a potentially confounding variable together with age, gender, and brain size. The results were almost the same as those without S as a covariate, but the *P*-value of group comparison of E_{global} between SZ and NC1 became smaller at almost all thresholds (Table S7). Therefore, our current findings are unlikely to be due to the potential global loss of connectivity in patients. In addition, all patients received antipsychotic treatment during the MRI scanning, and their effects may be a confounding factor in our findings. However, abnormal white-matter connectivity has also been reported in drug-naïve patients[57]. Furthermore, we did not find significant correlations between antipsychotic medication doses and network measures (Fig. S1). Therefore, it is unlikely that the altered structural brain network in patients resulted from antipsychotic medication alone. However, appropriately designed studies set up to specifically identify the effect of medication on structural network topology are needed.

There are some limitations in our study. First, issues derived from our special sample of participants need to be considered. As is often the case in a family study, there may be some heterogeneity of genetic predisposition to schizophrenia in first-degree relatives[58]. To distill this kind of heterogeneity, an obligate carrier study in which the unaffected relatives who appear to transmit a genetic predisposition to their affected children are classified as presumed obligate carriers, has been proposed[59]. However, such classification requires a large sample of multiply affected families. In our study, we had to lay aside classification of the parents of schizophrenic patients due to our limited sample size. In addition, two unrelated groups of healthy controls were separately recruited to match the affected families, which is a common practice in first-degree relative studies of schizophrenia. The family *versus* non-family design of our study may

weaken the interpretation of our findings. Second, we assessed the cognitive impairment of patients with the cognition score from PANSS. As discussed above, this score is known to accurately predict the daily activities of patients, but future studies with cognition assessment using neuropsychological tests or cognitive tasks will also be necessary to confirm our findings. Third, in our study, the anisotropic voxels of DTI data were acquired because we attempted to retain whole-brain coverage in a shorter scanning time for the schizophrenic patients, while keeping a reasonably small in-plane resolution. However, although the anisotropic voxels of DTI data are commonly used[34, 60], it should be noted that their use may partially impact the accuracy of the directionality of the diffusion tensor[61-63]. In a future study, we will use isotropic voxel sizes to ensure the accuracy of the fiber tractography.

In conclusion, the present study provides further evidence that the structural brain network is disturbed in schizophrenia and the global efficiency loss in neuroanatomical networks may be associated with the cognitive impairment in this disorder. The preliminary findings of node-specific network metrics changes in patients and their unaffected parents suggest that the anatomical network may be related to familial vulnerability of schizophrenia.

ELECTRONIC SUPPLEMENTARY MATERIAL

Supplementary material is available in the online version of this article at http://dx.doi.org/10.1007/s12264-014-1518-0.

ACKNOWLEDGEMENTS

This work was supported by grants from the National Basic Research Program of China (2011CB707805), the National Natural Science Foundation of China (81370032, 91232305, 81361120395, and 91432304), and the International Science & Technology Cooperation Program of China (2010DFB30820).

Received date: 2014-10-15; Accepted date: 2015-01-14

REFERENCES

[1] Bullmore E, Sporns O. Complex brain networks: graph theoretical analysis of structural and functional systems. Nat Rev Neurosci 2009, 10: 186–198.

[2] Bassett DS, Bullmore ET. Human brain networks in health and disease. Curr Opin Neurol 2009, 22: 340–347.

[3] Watts DJ, Strogatz SH. Collective dynamics of 'small-world' networks. Nature 1998, 393: 440–442.

[4] Sporns O, Chialvo DR, Kaiser M, Hilgetag CC. Organization, development and function of complex brain networks. Trends Cogn Sci 2004, 8: 418–425.

[5] Achard S, Bullmore E. Efficiency and cost of economical brain functional networks. PLoS Comput Biol 2007, 3: e17.

[6] Liu Y, Liang M, Zhou Y, He Y, Hao Y, Song M*, et al.* Disrupted small-world networks in schizophrenia. Brain 2008, 131: 945–961.

[7] Wang L, Metzak PD, Honer WG, Woodward TS. Impaired efficiency of functional networks underlying episodic memory-for-context in schizophrenia. J Neurosci 2010, 30: 13171–13179.

[8] Bassett DS, Bullmore E, Verchinski BA, Mattay VS, Weinberger DR, Meyer-Lindenberg A. Hierarchical organization of human cortical networks in health and schizophrenia. J Neurosci 2008, 28: 9239–9248.

[9] van den Heuvel MP, Mandl RC, Stam CJ, Kahn RS, Hulshoff Pol HE. Aberrant frontal and temporal complex network structure in schizophrenia: a graph theoretical analysis. J Neurosci 2010, 30: 15915–15926.

[10] Zalesky A, Fornito A, Seal ML, Cocchi L, Westin CF, Bullmore ET*, et al.* Disrupted axonal fiber connectivity in schizophrenia. Biol Psychiatry 2011, 69: 80–89.

[11] Konrad A, Winterer G. Disturbed structural connectivity in schizophrenia primary factor in pathology or epiphenomenon? Schizophr Bull 2008, 34: 72–92.

[12] Bullmore ET, Frangou S, Murray RM. The dysplastic net hypothesis: an integration of developmental and dysconnectivity theories of schizophrenia. Schizophr Res 1997, 28: 143–156.

[13] Friston KJ, Frith CD. Schizophrenia: a disconnection syndrome? Clin Neurosci 1995, 3: 89–97.

[14] Stephan KE, Baldeweg T, Friston KJ. Synaptic plasticity and dysconnection in schizophrenia. Biol Psychiatry 2006, 59: 929–939.

[15] Wang Q, Su TP, Zhou Y, Chou KH, Chen IY, Jiang T*, et al.* Anatomical insights into disrupted small-world networks in schizophrenia. Neuroimage 2012, 59: 1085–1093.

[16] Viding E, Williamson DE, Hariri AR. Developmental imaging genetics: challenges and promises for translational research. Dev Psychopathol 2006, 18: 877–892.

[17] Lawrie SM, McIntosh AM, Hall J, Owens DG, Johnstone EC. Brain structure and function changes during the development of schizophrenia: the evidence from studies of subjects at increased genetic risk. Schizophr Bull 2008, 34: 330–340.

[18] Hoptman MJ, Nierenberg J, Bertisch HC, Catalano D, Ardekani BA, Branch CA*, et al.* A DTI study of white

matter microstructure in individuals at high genetic risk for schizophrenia. Schizophr Res 2008, 106: 115–124.

[19] Camchong J, Lim KO, Sponheim SR, Macdonald AW. Frontal white matter integrity as an endophenotype for schizophrenia: diffusion tensor imaging in monozygotic twins and patients' nonpsychotic relatives. Front Hum Neurosci 2009, 3: 35.

[20] Hao Y, Yan Q, Liu H, Xu L, Xue Z, Song X*, et al*. Schizophrenia patients and their healthy siblings share disruption of white matter integrity in the left prefrontal cortex and the hippocampus but not the anterior cingulate cortex. Schizophr Res 2009, 114: 128–135.

[21] Knochel C, Oertel-Knochel V, Schonmeyer R, Rotarska-Jagiela A, van de Ven V, Prvulovic D*, et al.* Interhemispheric hypoconnectivity in schizophrenia: fiber integrity and volume differences of the corpus callosum in patients and unaffected relatives. Neuroimage 2012, 59: 926–934.

[22] Knochel C, O'Dwyer L, Alves G, Reinke B, Magerkurth J, Rotarska-Jagiela A*, et al*. Association between white matter fiber integrity and subclinical psychotic symptoms in schizophrenia patients and unaffected relatives. Schizophr Res 2012, 140: 129–135.

[23] Collin G, Kahn RS, de Reus MA, Cahn W, van den Heuvel MP. Impaired rich club connectivity in unaffected siblings of schizophrenia patients. Schizophr Bull 2014, 40: 438–448.

[24] Latora V, Marchiori M. Efficient behavior of small-world networks. Phys Rev Lett 2001, 87: 198701.

[25] Schmitt JE, Lenroot RK, Wallace GL, Ordaz S, Taylor KN, Kabani N*, et al.* Identification of genetically mediated cortical networks: a multivariate study of pediatric twins and siblings. Cereb Cortex 2008, 18: 1737–1747.

[26] Smit DJ, Stam CJ, Posthuma D, Boomsma DI, de Geus EJ. Heritability of "small-world" networks in the brain: a graph theoretical analysis of resting-state EEG functional connectivity. Hum Brain Mapp 2008, 29: 1368–1378.

[27] Oldfield RC. The assessment and analysis of handedness: the Edinburgh inventory. Neuropsychologia 1971, 9: 97–113.

[28] World Health Organization. The ICD-10 classification of mental and behavioural disorders : diagnostic criteria for research. Geneva: World Health Organization, 1993.

[29] Woods SW. Chlorpromazine equivalent doses for the newer atypical antipsychotics. J Clin Psychiatry 2003, 64: 663–667.

[30] Bai YM, Ting Chen T, Chen JY, Chang WH, Wu B, Hung CH*, et al.* Equivalent switching dose from oral risperidone to risperidone long-acting injection: a 48-week randomized, prospective, single-blind pharmacokinetic study. J Clin Psychiatry 2007, 68: 1218–1225.

[31] Lehman AF, Steinwachs DM. Translating research into practice: the Schizophrenia Patient Outcomes Research Team (PORT) treatment recommendations. Schizophr Bull 1998, 24: 1–10.

[32] Kay SR, Fiszbein A, Opler LA. The positive and negative syndrome scale (PANSS) for schizophrenia. Schizophr Bull 1987, 13: 261–276.

[33] Lindenmayer JP, Bernstein-Hyman R, Grochowski S. A new five factor model of schizophrenia. Psychiatr Q 1994, 65: 299–322.

[34] Li YH, Liu Y, Li J, Qin W, Li KC, Yu CS*, et al.* Brain anatomical network and intelligence. PLoS Comput Biol 2009, 5: e1000395

[35] Tzourio-Mazoyer N, Landeau B, Papathanassiou D, Crivello F, Etard O, Delcroix N*, et al.* Automated anatomical labeling of activations in SPM using a macroscopic anatomical parcellation of the MNI MRI single-subject brain. Neuroimage 2002, 15: 273–289.

[36] Gong GL, He Y, Concha L, Lebel C, Gross DW, Evans AC*, et al.* Mapping anatomical connectivity patterns of human cerebral cortex using in vivo diffusion tensor imaging tractography. Cereb Cortex 2009, 19: 524–536.

[37] Mori S, Crain BJ, Chacko VP, van Zijl PC. Three-dimensional tracking of axonal projections in the brain by magnetic resonance imaging. Ann Neurol 1999, 45: 265–269.

[38] Thottakara P, Lazar M, Johnson SC, Alexander AL. Application of Brodmann's area templates for ROI selection in white matter tractography studies. Neuroimage 2006, 29: 868–878.

[39] Gong G, Rosa-Neto P, Carbonell F, Chen ZJ, He Y, Evans AC. Age- and gender-related differences in the cortical anatomical network. J Neurosci 2009, 29: 15684–15693.

[40] Yu Q, Sui J, Rachakonda S, He H, Pearlson G, Calhoun VD. Altered small-world brain networks in temporal lobe in patients with schizophrenia performing an auditory oddball task. Front Syst Neurosci 2011, 5: 7.

[41] Li X, Xia S, Bertisch HC, Branch CA, Delisi LE. Unique topology of language processing brain network: A systems-level biomarker of schizophrenia. Schizophr Res 2012, 141: 128–136.

[42] Hagmann P, Cammoun L, Gigandet X, Meuli R, Honey CJ, Wedeen V*, et al.* Mapping the structural core of human cerebral cortex. PLoS Biol 2008, 6: 1479–1493.

[43] Crossley NA, Mechelli A, Scott J, Carletti F, Fox PT, McGuire P*, et al.* The hubs of the human connectome are generally implicated in the anatomy of brain disorders. Brain 2014, 137: 2382–2395.

[44] Lynall ME, Bassett DS, Kerwin R, McKenna PJ, Kitzbichler M, Muller U*, et al.* Functional connectivity and brain networks in schizophrenia. J Neurosci 2010, 30: 9477–9487.

[45] Supekar K, Menon V, Rubin D, Musen M, Greicius MD. Network analysis of intrinsic functional brain connectivity in Alzheimer's disease. PLoS Comput Biol 2008, 4: e1000100.

[46] Kalkstein S, Hurford I, Gur RC. Neurocognition in

schizophrenia. Curr Top Behav Neurosci 2010, 4: 373–390.

[47] Sheppard JP, Wang JP, Wong PC. Large-scale cortical network properties predict future sound-to-word learning success. J Cogn Neurosci 2012, 24: 1087–1103.

[48] Bassett DS, Bullmore ET, Meyer-Lindenberg A, Apud JA, Weinberger DR, Coppola R. Cognitive fitness of cost-efficient brain functional networks. Proc Natl Acad Sci U S A 2009, 106: 11747–11752.

[49] Velligan DI, Mahurin RK, Diamond PL, Hazleton BC, Eckert SL, Miller AL. The functional significance of symptomatology and cognitive function in schizophrenia. Schizophr Res 1997, 25: 21–31.

[50] Munoz Maniega S, Lymer GK, Bastin ME, Marjoram D, Job DE, Moorhead TW*, et al.* A diffusion tensor MRI study of white matter integrity in subjects at high genetic risk of schizophrenia. Schizophr Res 2008, 106: 132–139.

[51] Peters BD, de Haan L, Dekker N, Blaas J, Becker HE, Dingemans PM*, et al.* White matter fibertracking in first-episode schizophrenia, schizoaffective patients and subjects at ultra-high risk of psychosis. Neuropsychobiology 2008, 58: 19–28.

[52] Job DE, Whalley HC, Johnstone EC, Lawrie SM. Grey matter changes over time in high risk subjects developing schizophrenia. Neuroimage 2005, 25: 1023–1030.

[53] Harms MP, Wang L, Mamah D, Barch DM, Thompson PA, Csernansky JG. Thalamic shape abnormalities in individuals with schizophrenia and their nonpsychotic siblings. J Neurosci 2007, 27: 13835–13842.

[54] Glahn DC, Winkler AM, Kochunov P, Almasy L, Duggirala R, Carless MA*, et al.* Genetic control over the resting brain. Proc Natl Acad Sci U S A 2010, 107: 1223–1228.

[55] Fornito A, Zalesky A, Bassett DS, Meunier D, Ellison-Wright I, Yucel M*, et al.* Genetic influences on cost-efficient organization of human cortical functional networks. J Neurosci 2011, 31: 3261–3270.

[56] Seidman LJ, Faraone SV, Goldstein JM, Goodman JM, Kremen WS, Toomey R*, et al.* Thalamic and amygdala-hippocampal volume reductions in first-degree relatives of patients with schizophrenia: an MRI-based morphometric analysis. Biol Psychiatry 1999, 46: 941–954.

[57] Mandl RC, Rais M, van Baal GC, van Haren NE, Cahn W, Kahn RS*, et al.* Altered white matter connectivity in never-medicated patients with schizophrenia. Hum Brain Mapp 2013, 34: 2353–2365.

[58] Steel RM, Whalley HC, Miller P, Best JJ, Johnstone EC, Lawrie SM. Structural MRI of the brain in presumed carriers of genes for schizophrenia, their affected and unaffected siblings. J Neurol Neurosurg Psychiatry 2002, 72: 455–458.

[59] McDonald C, Grech A, Toulopoulou T, Schulze K, Chapple B, Sham P*, et al.* Brain volumes in familial and non-familial schizophrenic probands and their unaffected relatives. Am J Med Genet 2002, 114: 616–625.

[60] Bohlken MM, Mandl RC, Brouwer RM, van den Heuvel MP, Hedman AM, Kahn RS*, et al.* Heritability of structural brain network topology: a DTI study of 156 twins. Hum Brain Mapp 2014, 35: 5295–5305.

[61] Hasan KM, Walimuni IS, Abid H, Hahn KR. A review of diffusion tensor magnetic resonance imaging computational methods and software tools. Comput Biol Med 2011, 41: 1062–1072.

[62] Mukherjee P, Chung SW, Berman JI, Hess CP, Henry RG. Diffusion tensor MR imaging and fiber tractography: technical considerations. AJNR Am J Neuroradiol 2008, 29: 843–852.

[63] Oouchi H, Yamada K, Sakai K, Kizu O, Kubota T, Ito H*, et al.* Diffusion anisotropy measurement of brain white matter is affected by voxel size: underestimation occurs in areas with crossing fibers. AJNR Am J Neuroradiol 2007, 28: 1102–1106.